A new model to analyze the temperature effect on the microalgae performance at large scale raceway reactors

E. Rodríguez-Miranda,[†] F.G. Acién,[‡] J.L. Guzmán,[*,¶] M. Berenguel,[¶] and A. Visioli[†]

[†]*Department of Mechanical and Industrial Engineering, University of Brescia, 25123, Italy*

[‡]*Dep. de Ingeniería, Universidad de Almería, CIESOL, 04120 Almería, Spain*

[¶]*Dep. de Informática, Universidad de Almería, CIESOL ceiA3, 04120 Almería, Spain*

E-mail: joseluis.guzman@ual.es

Abstract

In this paper a simplified temperature model for raceway reactors is developed, allowing to determine the temperature of the microalgae culture as a function of reactor design and environmental conditions. The model considers the major phenomena taking place in raceway reactors, especially heat absorption by radiation and heat losses by evaporation among others. The characteristic parameters of the model have been calibrated using genetic algorithms, next being validated with a long set of more than 50 days covering different weather conditions. It is worth to highlight the use of the developed model as a tool to analyze the influence of the temperature on the performance of microalgae cultures at large scale. As example, the annual variation of the performance of up to five different microalgae strains has been determined by computing the temperature index, thus the normalized value of performance of whatever microalgae at the real temperature with respect to that achievable at optimal temperature can be established. Results confirm that only strains tolerant to wide ranges of temperature can be efficiently produced all the year around in large scale outdoor raceway reactors without additional temperature control systems.

Keywords: Biotechnology, Microalgae, Temperature model, Raceway reactor, Energy Balance.

Introduction

Nowadays, the implementation of microalgae reactors for biomass production is expanding due to the advantages and products that can be obtained from their exploitation. From microalgae biomass, high-value products can be obtained to be used in the chemical industry[1] or for animal food production, such as fish-food.[2] Another interesting type of application for microalgae biomass, which is currently under investigation, is the biofuel production.[3–6] On the other hand, the use of wastewater as a culture medium is allowing the development of new combined applications such as the simultaneous treatment and purification of water plus the production of biomass in a single process.[7] This solution is becoming popular because it allows reducing operating costs and enhancing the use of microalgae for low value applications, such as biofertilizers or bioenergy. The development of this type of applications is carried out in raceway reactors, which are the most extended type of reactors because they are less expensive and easy to operate than tubular-closed photobioreactors.

In addition to nutrient supply, the most relevant variables influencing the microalgae production processes are temperature, solar radiation, pH, and dissolved oxygen.[8,9] Temperature and solar radiation are mainly a function of the location where the reactor is installed and the season of the year. The variables to be controlled are pH and dissolved oxygen, in order to maintain them at specific operating levels despite changes in disturbances, such as solar radiation.[10] For that reason, detailed models for the pH and dissolved oxygen evolution in raceway photobioreactors can be found in literature.[11,12] Notice that the culture temperature could also be controlled by using solutions based on heat exchangers or external boilers, but this option is omitted because it increases on the operation costs. However, it is important to have dynamical models for the culture temperature evolution in photobiorectors that can be used as reactor design tools or for strain selection based on the reactor location.

Biological microalgae models can help to estimate and maximize crop productivity,[13] as well as characteristic parameters that can be used in control systems to maximize biomass production.[8,10,14] However, although there exist some studies combining the microalgae productivity and

culture temperature,[15,16] most existing biological models do not take the culture temperature into account, what is a limiting factor in the analysis of the microalgae productivity results.[17–20] Béchet *et al.* presented a universal temperature model for open reactors,[21] which makes use of dimensionless parameters for heat transfer and evaporation phenomena. The evaporation phenomenon is a complex process and difficult to estimate. In[22] a comparison of different evaporation models is presented. On the other hand, in,[23] a dynamic model for the cultivation of microalgae is developed where an empirical temperature model based on thermal energy balances suggested in[24] is included. These studies demonstrated the importance of temperature on microalgae growth and the complexity of accurately estimating its value. The combination of a temperature model with the current microalgae growth models would allow a greater accuracy in the representation of the microalgae behaviour. Thanks to this combination, better control architectures for biomass production and associated applications could be developed.

In this article, a new simple temperature model is presented, based on a review of the empirical relationships defined by Béchet *et al.* and Slegers *et al.* in,[21,24] and adapted to a raceway reactor. The culture temperature is calculated from a thermal balance in the reactor, taking into account all available environmental variables. This model allows the estimation of the temperature of the culture in the reactor for certain environmental conditions. In this way, the model could estimate parameters of interest, such as the time of harvest or anticipate risk temperatures that can negatively affect the crop. In addition, the model may be used to analyse the temperature impact on biomass production for different locations. In this way, design tools could be developed to study the viability of the microalgae production zones to determine the most suitable cultivation strains. Moreover, the temperature model can be used to improve existing microalgae estimation models or biomass growth models, such as those presented in[11] and.[25] Also, the temperature model can be used when there is a lack of temperature measurements in the reactor, being used as a temperature estimator.

The article is divided in the following way. Section 2 presents the reactor that was used to collect the real data and to validate the models. In Section 3, the components of the thermal

(a) Real raceway reactor.

(b) Reactor scheme.

Figure 1: Raceway reactor and structure scheme.

balance and the temperature model are detailed. Section 4 presents the results obtained using the temperature model, along with an analysis of how temperature influences five microalgae strains by using the temperature model and the growth rate model. Finally, Section 5 states the conclusions.

Material and methods

This section presents detailed information about the reactor, as well as the microalgae cultivated strain and the measurements.

Raceway reactor

The microalgae raceway reactor used for the test (Figure 1a) is located at the IFAPA centre, next to the University of Almería (Almería, Spain). The reactor has a total surface of 80 m^2, composed of two 80 m length channels connected by a 1 m wide U-shaped bends. Mixing is performed by a paddlewheel of aluminum blades with a diameter of 1.5 m, driven by an electric motor (W12 35 kW, 1500 rpm, Ebarba, Barcelona, Spain), with gear reduction (WEB Ibérica S.A., Barcelona, Spain). The paddlewheel speed is controlled with a frequency inverter (CFW 08 WEB Ibérica, S.A., Barcelona, Spain) at a constant velocity of 0.2 m/s. Carbonation is performed in a sump located 1.8 m downstream of the paddlewheel, which dimensions are 1.0 m depth, 0.65 m length and 1.0 m width. In this sump, CO_2 gas or air can be injected through three plate membrane

diffusers at the bottom of the sump (AFD 270, EcoTec, Spain). The raceway channels are made of low density polyethylene of 3 *mm* thickness while the curves and sump are made of high density polyethylene of 3 *mm* thickness.

In the reactor, there are five pH probes, five dissolved oxygen probes, and 5 temperature probes. Figure 1b shows a scheme of the system, where each red point consists of a sensor set that includes pH, dissolved oxygen, and temperature probes. Points one, two and three contain probes from Crison, while points four and five contain probes from Hamilton.

The measurements of the climatic conditions are obtained from a meteorological station, while the temperature of the soil and the depth of the culture are measured with sensors incorporated in the raceway reactor itself. Table 1 shows the model of the sensors for the measurable variables, which represent the inputs to the temperature model. The sampling period for the measurements is one second.

Table 1: Measuring sensors

Measure	**Model**
Wind speed	Anemometer Thies Clima 4.3400.30.000
Global solar irradiance	Pyranometer Kipp & Zonen CM 6B
Ambient temperature and humidity	Sensor Delta Ohm HD 9008TRR
Culture and soil temperature	Transducer PT100 with signal conditioner
Culture depth	Ultrasound sensor Wenglor UMD402U035

Microalgae strain

The microalgae strain used in the reactor belongs to *Scenedesmus almeriensis* (CCAP 276/24) species. A detailed study about its characteristic parameters and conditions related to pH, dissolved oxygen and temperature can be found in.[26] The pH value ranges from 3 up to 10, but the net photosynthesis rate is close to the maximal value from 5.7 to 8. Regarding the temperature, the value ranges from 12 to 46 $^{\circ}C$, but the optimum range is around 30 $^{\circ}C$. The culture medium used in the growth of the microalgae has been freshwater and Mann & Myers medium prepared using fertilizers (0.14 $g \cdot L^{-1}$ $K(PO_4)_2$, 0.18 $g \cdot L^{-1}$ $Mg(SO_4)_2$, 0.9 $g \cdot L^{-1}$ $NaNO_3$, 0.02 $mL \cdot L^{-1}$ Welgro,

and 0.02 $g \cdot L^{-1}$ Kalentol).[27]

Thermal balance and temperature model

The thermal balance described in this paper is based on first principles and empirical equations defined for the transfer of energy due to solar irradiance, long wave radiation, evaporation, convection, and conduction.

Based on the models described in,[21,24] the energy balances that affect the culture have been analysed and established, and a new thermal balance has been developed to estimate the culture temperature in the reactor from measurable variables. The solar irradiance input comes from data measured by the global (direct + diffuse) radiation sensor mentioned above. Long-wave radiation losses are calculated by the Stefan-Boltzmann Law ([28]). There are different methodologies in the literature to obtain the evaporation flow[21].In this case, the energy balance by evaporation is calculated from the evaporation rate obtained from an experimental evaporation exchange coefficient. Convection is expressed by Newton's Law of cooling, and finally, conduction is expressed as the heat transfer between the mass of the culture in the reactor and the polyethylene layer that insulates the reactor from the ground. As a result of the introduced energy balances, the thermal balance is expressed by the following equation (Q_i in W):

$$Q_{accumulated} = Q_{irradiance} + Q_{radiation} + Q_{evaporation} + Q_{convection} + Q_{conduction} \tag{1}$$

where $Q_{accumulated}$ is the heat accumulated in the reactor, $Q_{irradiance}$ represents the flow of heat from sunlight, $Q_{radiation}$ is the long-wave radiation heat flow, $Q_{evaporation}$ accounts for the heat flow produced by the evaporation process, $Q_{convection}$ is the heat flow caused by convection and $Q_{conduction}$ represents the heat flow between the reactor and the polyethylene layer under it through a conduction process.

Accumulated heat flow

The heat accumulated in the reactor represents the sum of all energy terms that affect the reactor, and it is expressed by the following equation:

$$Q_{accumulated} = h \cdot A \cdot C_p \cdot \rho \cdot \frac{dT_w}{dt} \tag{2}$$

with h (m) the culture depth, A (m^2) the surface of the reactor, C_p $(J\ kg^{-1}\ {}^{\circ}C^{-1})$ the specific heat capacity of the culture, ρ $(kg\ m^{-3})$ the density of the culture and T_w $({}^{\circ}C)$ the temperature of the culture in the reactor.

Heat flow due to the effect of solar irradiance

The heat flow due to incident solar irradiance on the reactor surface represents the main heat input into the reactor. It is expressed by the following equation:

$$Q_{irradiance} = I_g \cdot a \cdot A \tag{3}$$

where I_g $(W\ m^{-2})$ is the global (direct + diffuse) solar irradiance, a $(-)$ is the absorptivity, and A (m^2) represents the total area of the reactor.

Radiation heat losses

The reactor emits thermal energy as long-wave radiation. The flow of radiated energy between the reactor and the sky is calculated using the following equation:

$$Q_{radiation} = \sigma \cdot A \cdot e \cdot \left({T_{sky}}^4 - (T_w + 273.15)^4 \right) \tag{4}$$

with σ $(W\ m^{-2}\ K^{-4})$ the Stefan-Boltzmann constant, e $(-)$ the water emissivity and T_{sky} (K) the equivalent temperature of the sky, expressed in ([28]) with the following expression:

$$T_{sky} = (273.15 + T_{amb})(0.711 + 0.0056 \cdot T_{dew} \cdot 0.000073 \cdot T_{dew}^2 + 0.13 \cdot \cos(15 \cdot t_{solar}))^{0.25} \quad (5)$$

where T_{amb} $(^{\circ}C)$ is the ambient temperature, T_{dew} $(^{\circ}C)$ the dew point temperature, and t_{solar} $(-)$ represents the number of hours after midnight.

Evaporation heat flow

The evaporation process represents the main source of heat loss in the reactor and depends on the shape of the reactor, the evaporation rate and the latent heat of vaporization, as presented in ([29]). The evaporation heat flow is determined as follows:

$$Q_{evaporation} = A \cdot E_p \cdot \rho \cdot h_{fg} \quad (6)$$

where E_p $(m\ s^{-1})$ is the evaporation rate, ρ $(kg\ m^{-3})$ is the density of the culture and h_{fg} $(J\ kg^{-1})$ is the latent heat of vaporization, expressed as follow:

$$h_{fg} = (2494 - 2.2 \cdot T_w) \cdot 1000 \quad (7)$$

The evaporation rate can be calculated as an empirical equation which depends on the difference in vapour pressures between the ambient air and the reactor culture mass ([29,30]), in addition to an evaporation exchange coefficient which depends on wind speed W_s:

$$E_p = \left(\frac{RH \cdot p'_A}{100} - p'_A \right) \cdot h_{evap} \quad (8)$$

where RH $(\%)$ is the relative humidity, p'_A (Pa) is the vapor pressure of the air at ambient temperature and h_{evap} $(m\ s^{-1}\ Pa^{-1})$ is an evaporation exchange coefficient, obtained experimentally from the following equation:

$$h_{evap} = A_{evap} + B_{evap} \cdot W_s \tag{9}$$

where W_s $(m\ s^{-1})$ is the wind speed and A_{evap} and B_{evap} are evaporation experimental coefficients that must be calibrated (with adequate units).

For the calculation of the vapour pressure of the environment at ambient temperature p'_A (kPa), the Tetens equation[31,32] has been used:

$$p'_A = 0.61078 \cdot exp\left(\frac{12.27 \cdot T_{amb}}{T_{amb} + 237.3}\right) \tag{10}$$

Convection heat flow

The phenomenon of convection occurs between the mass of water in the reactor and the air in the environment, resulting in a positive or negative balance depending on the moment of the day and the ambient temperature. The convection balance is represented by the following equation:

$$Q_{convection} = h_{conv} \cdot A \cdot (T_{amb} - T_w) \tag{11}$$

where T_{amb} $(^\circ C)$ is the ambient temperature and T_w $(^\circ C)$ is the temperature of the culture in the reactor and h_{conv} $(W\ m^{-2}\ ^\circ C^{-1})$ is the convection transfer coefficient, obtained experimentally as previously done for the evaporation:

$$h_{conv} = A_{conv} + B_{conv} \cdot W_s \tag{12}$$

with A_{conv} and B_{conv} experimental coefficients that must be calibrated.

Heat flow by conduction

The thermal conduction balance represents the thermal exchange between the reactor and the surface under it. Notice that polyethylene was the material used for the construction of the bottom of the reactor. So, the following equation represents the conduction balance:

$$Q_{conduction} = h_{soil} \cdot A_{soil} \cdot (T_{soil} - T_w) \tag{13}$$

where h_{soil} $(W\ m^{-2}\ ^{\circ}C^{-1})$ is the heat transfer coefficient for the layer, A_{soil} (m^2) is the surface of the reactor in contact with the ground and T_{soil} $(^{\circ}C)$ represents the temperature under the polyethylene layer of the reactor. The transfer coefficient h_{soil} can be expressed as follows:

$$h_{soil} = \frac{K_{soil}}{x_{soil}} \tag{14}$$

where K_{soil} $(W\ m^{-1}\ ^{\circ}C^{-1})$ is the conduction transfer coefficient for the polyethylene layer (calibration parameter) and x_{soil} (m) represents the distance between the bottom of the reactor and the buried temperature probe.

Temperature model

The model depends on a series of environmental input variables that are solar irradiance, ambient temperature, relative humidity and wind speed. Other input variables are culture depth and soil temperature, which can be easily estimated or approximated, instead of measured. Specifically, the depth of the culture can be set to its common value and the temperature of the soil under the reactor can be estimated based on the ambient temperature or set to a constant value. In this way, only the measurements of the environmental variables would be needed to run the model and use it as a temperature estimator.

The dynamic evolution of culture temperature is obtained from equation (1), based on the thermal balances described and reformulated as the following equation:

$$\frac{dT_w}{dt} = \frac{Q_{irradiance} + Q_{radiation} + Q_{evaporation} + Q_{convection} + Q_{conduction}}{h \cdot A \cdot C_p \cdot \rho} \tag{15}$$

Table 2 contains the description and the values of all the parameters used in the thermal balance of the temperature model, separated by constant and variable parameters.

Table 2: Parameters description

Parameter	Description	Value	Unit
Constants			
A	Surface of the reactor	80	$[m^2]$
C_p	Specific heat capacity of the culture	4184	$[J\ kg^{-1}\ {}^{\circ}C^{-1}]$
ρ	Density of the culture	1000	$[kg\ m^{-3}]$
a	Absorptivity	0.7	$[-]$
σ	Stefan–Boltzmann constant	$5.6697 \cdot 10^{-8}$	$[W\ m^{-2}\ K^{-4}]$
e	Water emissivity	0.9	$[-]$
A_{evap}	Evaporation experimental coefficient A	$1.20 \cdot 10^{-11}$	$[-]$
B_{evap}	Evaporation experimental coefficient B	$4.67 \cdot 10^{-12}$	$[-]$
A_{conv}	Convection experimental coefficient A	4.78	$[-]$
B_{conv}	Convection experimental coefficient B	6.83	$[-]$
K_{soil}	Conduction transfer coefficient for the polyethylene layer	0.43	$[W\ m^{-1}\ {}^{\circ}C^{-1}]$
x_{soil}	Thickness of the polyethylene layer of the reactor	0.02	$[m]$
A_{soil}	Surface of the reactor in contact with the ground	80	$[m^2]$
Variables			
h	Medium depth	–	$[m]$
T_w	Temperature of the culture	–	$[^{\circ}C]$
I_g	Global solar irradiance	–	$[W\ m^{-2}]$
T_{sky}	Temperature of the sky	–	$[^{\circ}C]$
T_{amb}	Ambient temperature	–	$[^{\circ}C]$
T_{dew}	Dew point temperature	–	$[^{\circ}C]$
t_{solar}	Number of hours after midnight	–	$[-]$
h_{fg}	Latent heat of vaporization	–	$[J\ kg^{-1}]$
E_p	Evaporation rate	–	$[m\ s^{-1}]$
RH	Relative humidity	–	$[\%]$
p'_A	Vapor pressure of the air at ambient temperature	–	$[Pa]$
h_{evap}	Evaporation exchange coefficient	–	$[m\ s^{-1}\ Pa^{-1}]$
W_s	Wind speed	–	$[m\ s^{-1}]$
h_{conv}	Convection transfer coefficient	–	$[W\ m^{-2}\ {}^{\circ}C^{-1}]$
T_{soil}	Soil temperature	–	$[^{\circ}C]$

Results and discussion

This section presents the results obtained from the temperature model in three parts: a first part where the calibration process is shown; a second part presenting the results for the validation stage; and a third part where an analysis of how temperature influences five strains of microalgae is presented, using the temperature model.

Calibration

The equations developed in Section 3 make use of a series of parameters whose exact values are unknown, or the values are known in a defined range. The uncertainty in the value of these parameters shows the need for a calibration process, which has been carried out through genetic algorithms. Calibration using genetic algorithms results in an useful and reliable method in the estimation of uncertain parameters, since it allows optimizing a certain cost function that measures the deviation of the output of the model from that of the real system by modifying the parameter values between the established limits. The range of the estimated parameters has been obtained from the cited literature, as well as from the experience in the design of the installation.

The calibration process using genetic algorithms has been implemented in Matlab using the Genetic Algorithm Optimization Toolbox (GAOT), based on ([33]), with an initial population of 50 phenotypes (solutions) and a termination condition of 50 generations. This method starts with an initial set of calibration parameters and runs the model to obtain the error. The cost function is computed as the Root Mean Square Error (RMSE) between the simulated temperature and the real reactor temperature, expressed as the following equation:

$$J = \sqrt{\sum_{i=1}^{N} \frac{(T_{sim}(i) - T_{real}(i))^2}{N}} \tag{16}$$

where T_{sim} $(^{\circ}C)$ is the estimated temperature, T_{real} $(^{\circ}C)$ is the real culture temperature in the reactor and N (s) represents the size of the data vector.

The method modifies the calibration parameters in each iteration of the genetic algorithm in the

simulation as new population generations, within established limits, until the error cost function is minimized.

Three consecutive days from every month between August to December (15 days in total) have been used by the genetic algorithm to estimate the values of the calibration parameters trying to capture the different season dynamics. The data used for calibration purposes, which represent the input variables for the model (solar irradiance, ambient temperature, soil temperature, wind speed, the relative humidity and the culture depth), are shown in Figure 2 and separated by colours for each different month. As can be seen, there exist a large variability in the climatic data.

Table 3 presents the values of the calibration parameters obtained using the calibration data set. The evaporation (A_{evap} and B_{evap}) and convection (A_{conv} and B_{conv}) coefficients depend on the wind speed and the conduction coefficient (K_{soil} [$W\ m^{-1}\ ^{\circ}C^{-1}$]) ranges from 0.33 to 0.50 due to the polyethylene thermal conduction coefficient.

Table 3: Calibration parameters

Symbol	**Parameter**	**Value**	**Unit**
A_{evap}	*Evaporation coefficient parameter A*	$1.20 \cdot 10^{-11}$	[–]
B_{evap}	*Evaporation coefficient parameter B*	$4.67 \cdot 10^{-12}$	[–]
A_{conv}	*Convection coefficient parameter A*	4.78	[–]
B_{conv}	*Convection coefficient parameter B*	6.83	[–]
K_{soil}	*Conduction coefficient*	0.43	[$W\ m^{-1}\ ^{\circ}C^{-1}$]

The calibration results are shown in Figure 3, where the results of each month are individually plotted in different colors for better visualization. The differences between the temperature from one month to another is clearly visible, and the model is able to capture the temperature dynamics during the whole day, in addition to adjusting to the ranges of each month. The RMSE value obtained is 0.97 [$^{\circ}C$], while the mean temperature error is 0.85 [$^{\circ}C$], which is a satisfactory result, in addition to a maximum temperature error of 2.36 [$^{\circ}C$], occurring during the November nights.

If the results of each month are analyzed, it can be seen how the dynamics of the model re-

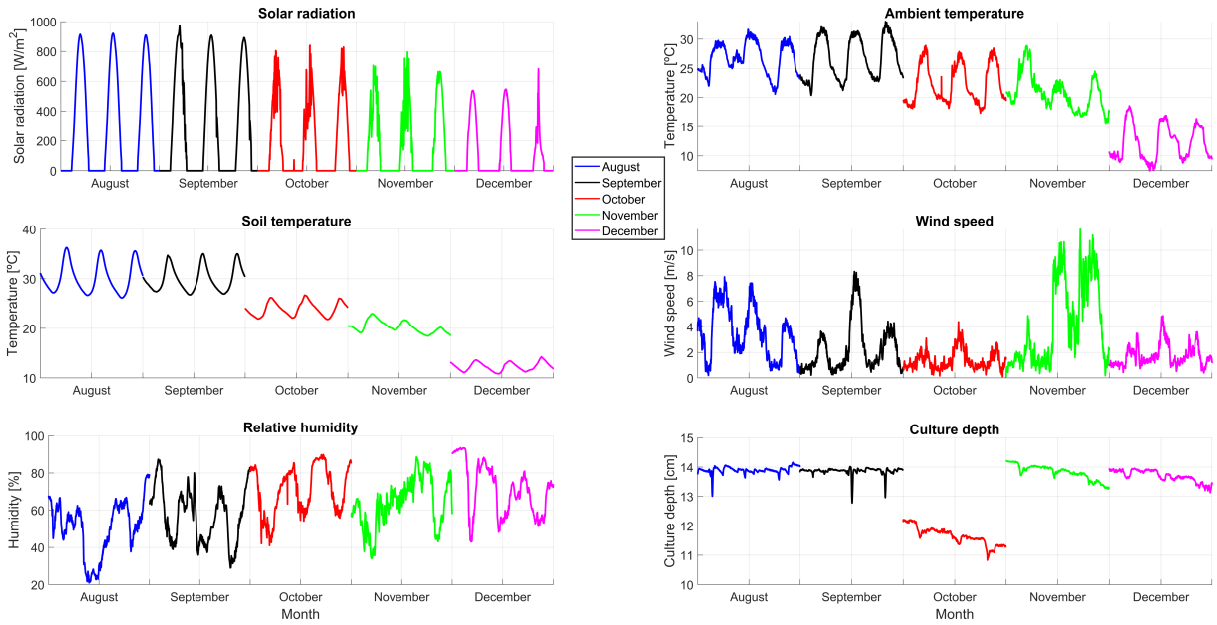

Figure 2: Environmental input variables for calibration. Every color represents three consecutive days of the month from August to December. For the correct visualization of the colors in the graphs, refer to the web version of the paper.

sembles the real temperature in the raceway reactor during all months. Although the dynamics and the maximum and minimum temperatures of each month vary, the model fits the real evolution in all cases, estimating the temperature satisfactorily. For the months of August, September and October, the model correctly estimates the culture temperature in the reactor, with an average error of 0.6 [$^{\circ}C$]. However, for the cold months of November and December, the model presents a little bit more errors, especially at night, with a mean error of 1.1 [$^{\circ}C$] for those months. Anyway, the relevant dynamics of the temperature variable is captured.

Validation

For the validation of the model, a set of 50 days has been used, belonging to the months from August to December. This data set, presented in Figure 4, shows the entire range of temperatures that can occur in the year, from the high values of August to the low ones in December. The input data is grouped in 5 months with 10 consecutive days each, presented in different colors for a better visualization. The temperature differences are perfect to check the adaptability of the temperature

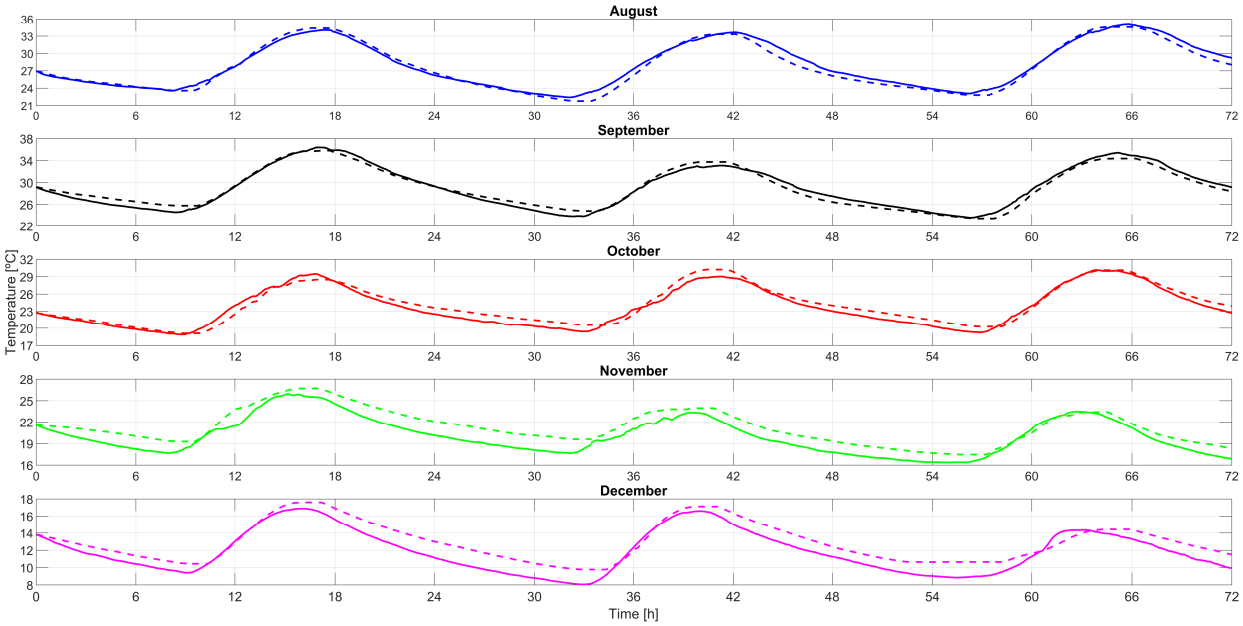

Figure 3: Temperature calibration results. Each individual color plot represents three consecutive days for the selected months from August to December. Dashed lines represent real reactor temperature while solid lines represent estimated temperature. For the correct visualization of the colors in the graphs, refer to the web version of the paper.

model and verify that it faithfully represents the dynamics of the system, regardless of the month. Figure 5 shows the validation results for the temperature model, where each month is represented individually following the same than for the calibration results. The model follows the dynamics of the culture temperature in the reactor, with a maximum error of 3.9 [$^{\circ}C$] and a mean error of 0.86 [$^{\circ}C$]. For the entire data set an RMSE value of 1.03 [$^{\circ}C$] has been obtained.

As in the calibration results shown in Figure 3, the estimated temperature for the months of August and September adequately resembles the real temperature of the reactor, with a mean error of 0.5 [$^{\circ}C$]. The results for the month of October during the daytime period are very satisfactory, however, during the nighttime there are certain discrepancies, increasing the mean error to 0.95 [$^{\circ}C$]. These errors, like in the last represented day of October, may be due to errors in the measurements of the input variables or isolated punctual phenomena that affect the temperature of the reactor. On the other hand, the months of November and December have a greater error (mean error of 1.15 [$^{\circ}C$]) in the estimation, although the dynamics resembles the real temperature and the results are satisfactory.

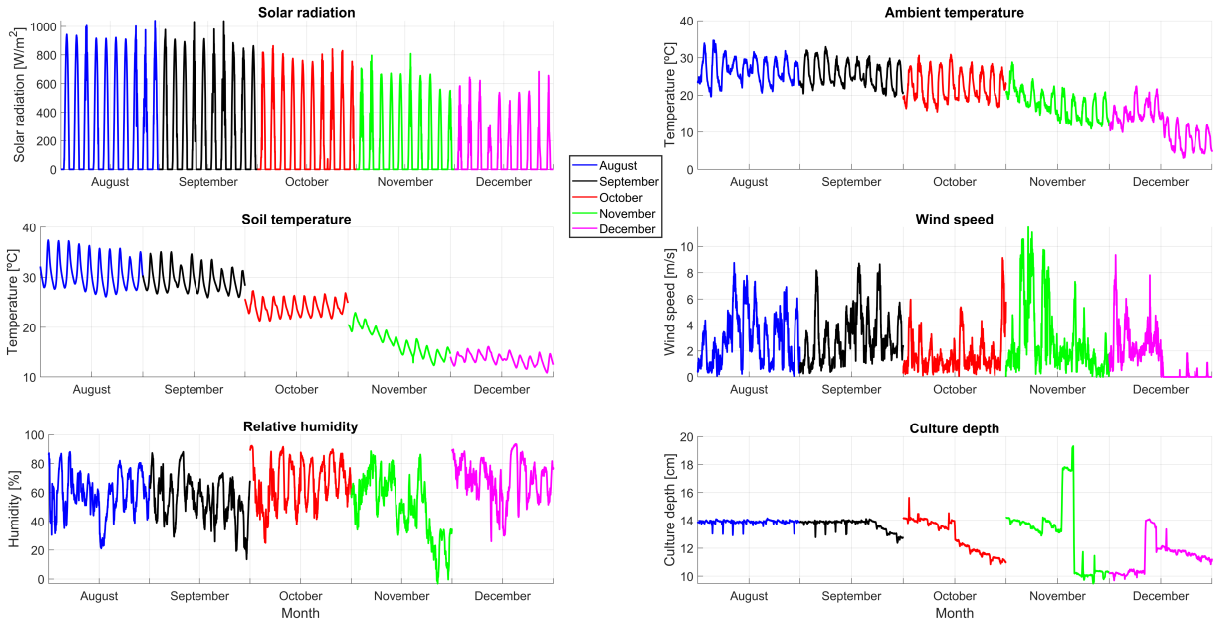

Figure 4: Environmental input variables for validation. Each month (from August to December) is represented by different colors and it is made up of 10 consecutive days each. For the correct visualization of the colors in the graphs, refer to the web version of the paper.

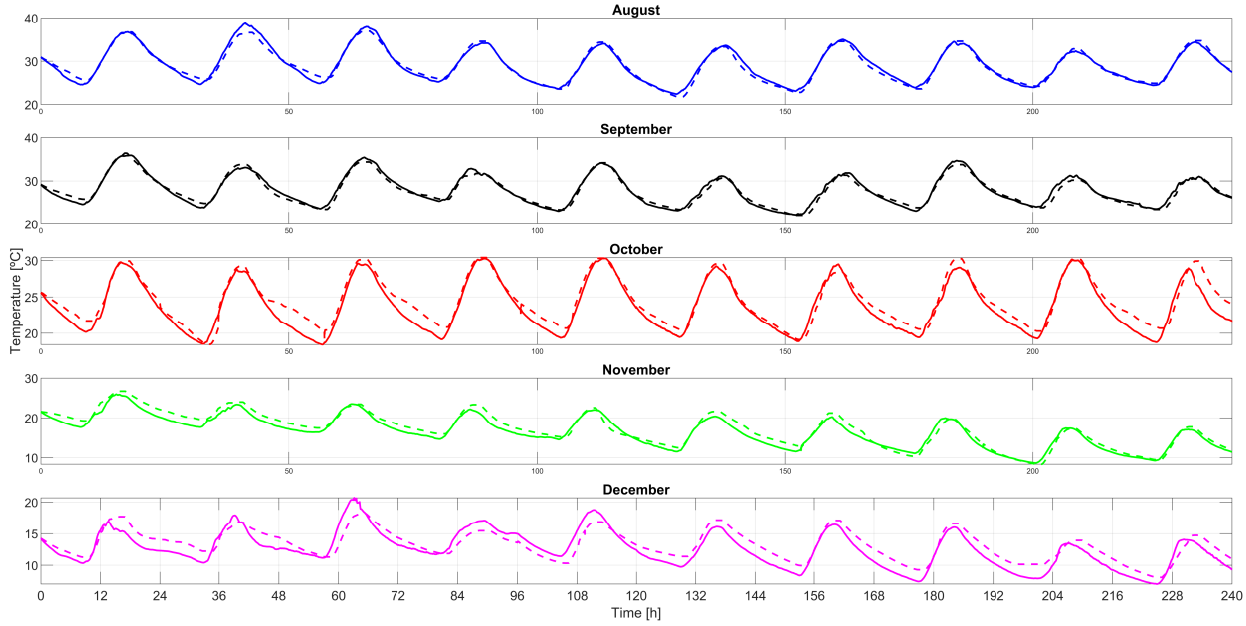

Figure 5: Temperature validation results. Every individual color plot represents ten consecutive days for the selected months from August to December. Solid line represents estimated temperature while dashed line represents real reactor temperature. For the correct visualization of the colors in the graphs, refer to the web version of the paper.

Temperature influence on microalgae activity for different strains

Using the developed temperature model, an analysis on how temperature influences on microalgae growth was carried out for five microalgae strains. For this issue, the temperature-effect on growth model presented by Bernard *et al.* in [16] was used together with the temperature model described in this paper.

The microalgae specific growth rate model has been used extensively in literature [16,26] and was formulated by Camacho-Rubio *et al.* in. [34] This model states that the microalgae growth rate, μ, is made up of four factors that depend on photosynthetically active radiation and light availability inside the culture (I_{av}), culture temperature (T_w), the pH, and the dissolved oxygen (DO) in the reactor. The growth model is described by the following equation:

$$\mu = \mu(I_{av}) \cdot \overline{\mu}(T_w) \cdot \overline{\mu}(pH) \cdot \overline{\mu}(DO) \tag{17}$$

The specific growth rate (μ) is mainly a function of light availability inside the reactor summarized by the average irradiance inside the culture (I_{av}) ([35]). This function is expressed as follows:

$$\mu(I_{av}) = \mu_{max} \cdot \left(\frac{{I_{av}}^n}{{I_k}^n + {I_{av}}^n} \right) \tag{18}$$

where μ_{max} $[day^{-1}]$ is the maximum growth rate, I_{av} $[\mu E\ m^{-2}\ s^{-1}]$ is the light availability inside the reactor summarized by the average irradiance inside the culture, I_k $[\mu E\ m^{-2}\ s^{-1}]$ is the minimum light needed by the microalgae to achieve maximum photosynthesis and n $[-]$ is a form parameter.

For a specific geometry, the average irradiance (I_{av}) is a function of the light path inside the culture, the biomass concentration and the extinction coefficient of the biomass. The specific growth rate hyperbolically increases with the average irradiance up to achieve the maximum specific growth rate μ_{max} for the selected strain. Whatever the microalgae strains, for any operational conditions a fix specific growth rate is achieved, being higher or lower according to the optimal value of other cultures parameters such as temperature, pH and dissolved oxygen among others.

The factors of temperature, pH and dissolved oxygen are normalized values and the overline

indicates that the term varies between 0 and 1, which multiply the solar radiation parameter. Therefore, when these three (T_w, pH and DO) parameters are optimal and have a value of 1, the specific growth rate only depends on solar radiation and would have the maximum possible value. However, if any of these parameters is not optimal, it would have a direct negative impact on the growth rate.

The temperature index ($\overline{\mu}(T_w)$) is a parameter that represents the influence of temperature on microalgae growth, directly related to biomass growth, where 1 means the maximum yield due to an optimal temperature of the culture. The biomass growth performance can be diminished by the effect of the temperature, therefore a temperature above or below the characteristic limits of the microalgae would result in null growth. For example, a strain that does not exceed a temperature index of 0.5 in a location means that at most, it is not capable of reaching half its maximum growth rate, so it would be limited to a great extent due to temperature conditions. Thus, the temperature index can be used independently to analyze the influence of temperature on microalgae strains, as it has a direct effect on the specific growth rate.

As commented above, the rest of factors in equation (17) are normalized factors that affects $\mu(I_{PAR})$. Specifically, the temperature index can be obtained from the following equation, based on the maximum (T_{max}), minimum (T_{min}) and optimum (T_{opt}) temperature values of the microalgae strain, shown in Table 4:

$$\overline{\mu}(T_w) = \frac{(T_w - T_{max}) \cdot (T_w - T_{min})^2}{(T_{opt} - T_{min}) \cdot ((T_{opt} - T_{min}) \cdot (T_w - T_{opt}) - (T_{opt} - T_{max}) \cdot (T_{opt} + T_{min} - 2 \cdot T_w))} \quad (19)$$

where T_w $[^{\circ}C]$ is the temperature of the culture, calculated with the temperature model described in equation (15).

The analysis has been done with representative data of 8 days of each seasonal period over a year at Almería, in Spain, characterized by moderate temperatures in summer and temperate in winter. The climate in Almería is considered a local steppe climate, with little rainfall. During the

course of the year, the temperature generally varies from 8 [$^{\circ}C$] to 30 [$^{\circ}C$] and rarely drops below 6 [$^{\circ}C$] or rises above 35 [$^{\circ}C$]. The objective has been to verify the influence of temperature on microalgae cultivation for five different species of microalgae throughout an annual period in this location. These microalgae species correspond to *Dunaliella tertiolecta*, *Nannochloropsis oceanica*, *Chlorella pyrenoidosa* and *Spirulina platensis*, being commonly used for biomass production at industrial scale, in addition to *Scenedesmus almeriensis*, the strain used in the raceway reactor studied. Table 4 represents the characteristic temperature parameters for each microalgae strain, applied to the temperature index model and obtained from the literature ([16,26]) and experimental tests in our research group. Despite the fact that the microalgae used in the reactor is *Scenedesmus almeriensis*, the temperature model is independent of the type of strain used, because it is a model to estimate the culture temperature. The characteristic temperature parameters for each strain are necessary in the cardinal model (equation 19), which in combination with the temperature model, allows to analyze its influence for any microalgae strain.

Table 4: Microalgae characteristic temperatures

Microalgae strain	T_{min} [°C]	T_{opt} [°C]	T_{max} [°C]
Scenedesmus almeriensis	12	30	46
Dunaliella tertiolecta	5	32.6	38.9
Nannochloropsis oceanica	-0.2	26.7	33
Chlorella pyrenoidosa	5.2	38.7	45.8
Spirulina platensis	7.7	37	50.6

Figure 6 represents the analysis carried out for the five types of microalgae during 8 days for each season of the year. The first five graphs represent the temperature factor ([16]) that affects the microalgae growth. The last graph at the bottom represents the estimated temperature in the raceway reactor for the entire data set using the temperature model. The ideal seasons to cultivate the microalgae *Scenedesmus almeriensis*, used in the reactor described in Section 2, are the last half of spring, the summer and the first half of autumn. However, during winter, the temperature index is practically 0, which denotes zero growth. The *Dunaliella tertiolecta* strain is resistant to medium/high temperatures and with a good temperature index late spring, summer and early autumn, while its performance can be diminished by the low temperatures of winter. The microalgae

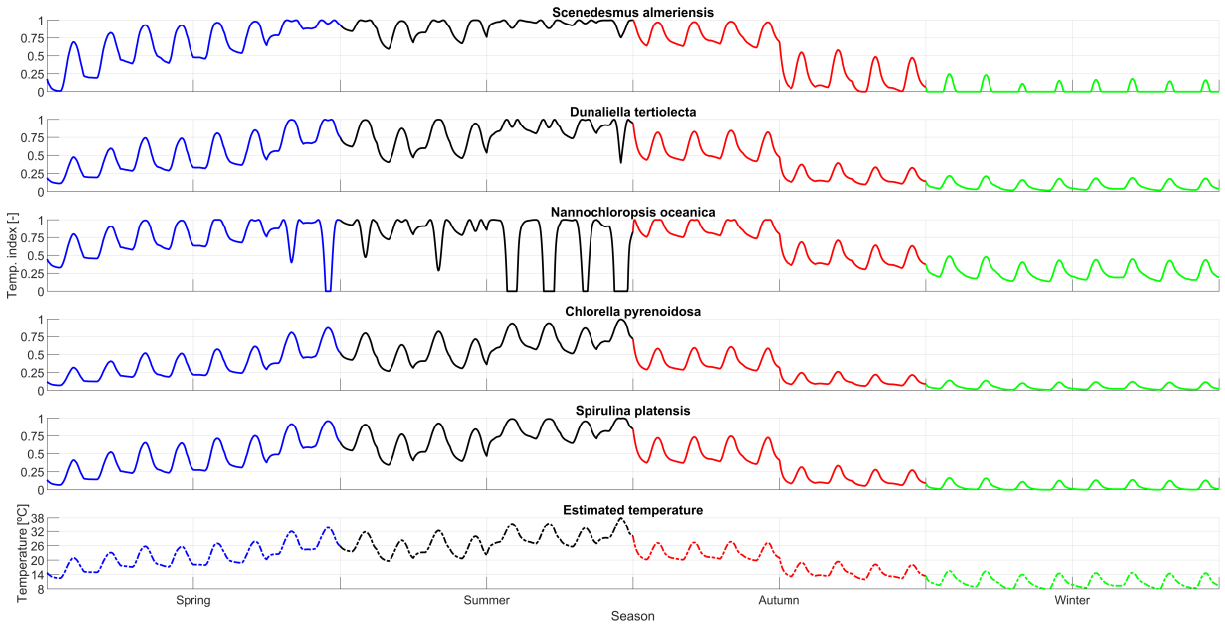

Figure 6: Temperature index analysis during seasonal periods. The results for the data set of eight days are represented individually and divided in four colours representing the different seasons. First graph corresponds to *Scenedesmus almeriensis*. Second graph corresponds to *Dunaliella tertiolecta*. Third graph corresponds to *Nannochloropsis oceanica*. Fourth graph corresponds to *Chlorella pyrenoidosa*, while fifth graph corresponds to *Spirulina platensis*. Sixth graph represents the estimated temperature in the raceway reactor (dashed line). For the correct visualization of the colors in the graphs, refer to the web version of the paper.

Nannochloropsis oceanica would not resist the summer period but it shows good results during the rest of the year, especially in winter, where its productivity exceeds the other strains analyzed. Both *Chlorella pyrenoidosa* and *Spirulina platensis* strains show a good temperature index during the summer period, together with late spring and the early autumn, as for *Dunaliella tertiolecta*, in contrast to practically no growth in winter due to low temperatures. The results obtained show a clear relationship with the characteristic values of each strain represented in Table 4 allowing an estimation of the viability of each strain for the studied location.

Discussion

The error obtained in Figures 3 and 5 denotes a promising accuracy in the model obtained from thermal balances. From the biological point of view, the error related to the estimated and the actual temperature would not be a problem according to the global process dynamics. The model is able

to accurately represent the temperature during the whole day. However, notice that in some days the error is larger than in others. These mismatches may be due to the existence of non-measurable terms or disturbances that have not been contemplated in the thermal balances, such as punctual errors in the measurements, irregular operations in the reactor or temperature of culture medium for replacement. On the other hand, the calibration by means of genetic algorithms allows to obtain mean values of parameters used in the equations that are subjected to uncertainty, as they are in lumped-parameters representations of balances that should require distributed parameter representations and thus are in general difficult to obtain from tables. In general, the results obtained have been positive and notable for the use of the model in the development of microalgae growth models where its dynamics and other parameters such as productivity, performance, consumption of CO_2, and evolution of pH are estimated.

The results of the temperature analysis for the cultivation of microalgae in Almería using the temperature model for raceway reactors have determined that *Scenedesmus almeriensis* and *Dunaliella tertiolecta* microalgae are suitable for production during most part of the year, especially during summer, due to its high temperature index. Both *Chlorella pyrenoidosa* and *Spirulina platensis* strains are also suitable for cultivation during the spring, summer and autumn periods, due to a good temperature index behaviour but less suitable than those described above. On the other hand, the microalgae *Nannochloropsis oceanica* is not capable of withstanding the temperatures reached during late spring and summer periods, being a microalgae difficult to cultivate in these periods, but being the most suitable for cultivation in autumn and winter because it shows the highest temperature index of all strains for this seasonal period.

The environmental conditions depend on the weather and can be very different from one season to another. This fact has been taken into account in the calibration of the model so that it can adjust to all the environmental conditions of each month, without changing the parameters or increasing the model complexity. On the other hand, being a model designed for all months of the year, there are certain errors due to a generalization of parameters, but a tradeoff between performance and complexity has been found.

The temperature estimation is really useful in the microalgae production process. The temperature model can be combined with existing microalgae biomass production models to add the effect of temperature on growth and thus make more accurate and complete microalgae production models. On the other hand, temperature estimation can be used as a design tool when installing a reactor in a determined location. From the growth productivity model and the environmental conditions, it is possible to estimate the temperature of a reactor in that area and establish its maximum biomass production or the microalgae strain viability. In this way, it is possible to assess the suitability to install a raceway reactor in any specific area or establish different microalgae cultures depending on the season. Moreover, it can also be used to design control algorithms to optimize the reactor temperature.

Conclusions

This work presents a temperature model for raceway reactors based on a thermal balance from measurable conditions in the environment. The results of the dynamic temperature evolution obtained from the model show satisfactory performance that closely resemble the actual temperature values, measured in the reactor. The great impact of temperature on the productivity of microalgae has been demonstrated in the literature and, therefore, this type of models has a fundamental role in the development of new and more complete models of microalgae that allow us to fully understand all the parameters that affect its growth. The use of industrial scale models that take into account all the variables affecting the microalgae growth is scarce in practice, and thus, this temperature model aims to complement the use of more complete models that allow the development of precise evaluation applications in the field of microalgae, such as optimal reactor control, variable impact studies, performance improvement or parameter estimation. In future work, the usefulness of the model to estimate the productivity of microalgae from different conditions will be analyzed, in addition to its use as a design tool.

Acknowledgement

This work has been partially funded by the following projects: DPI2017 84259-C2-1-R (financed by the Spanish Ministry of Science and Innovation and EU-ERDF funds), and the European Union's Horizon 2020 Research and Innovation Program under Grant Agreement No. 727874 SABANA.

References

(1)Hempel, N.; Petrick, I.; Behrendt, F. Biomass productivity and productivity of fatty acids and amino acids of microalgae strains as key characteristics of suitability for biodiesel production. *Journal of Applied Phycology* **2012**, *24*, 1407–1418.

(2)Wolfgang, B. Microalgae for Aquaculture: The Nutritional Value of Microalgae for Aquaculture. *Handbook of Microalgal Culture: Biotechnology and Applied Phycology* **2004**,

(3)Rodolfi, L.; Chini Zittelli, G.; Bassi, N.; Padovani, G.; Biondi, N.; Bonini, G.; Tredici, M. R. Microalgae for oil: strain selection, induction of lipid synthesis and outdoor mass cultivation in a low-cost photobioreactor. *Biotechnology and Bioengineering* **2009**, *102*, 100–112.

(4)Moody, J. W.; McGinty, C. M.; Quinn, J. C. Global evaluation of biofuel potential from microalgae. *Proceedings of the National Academy of Sciences of the United States of America* **2014**, *111*, 8691 - 8696.

(5)del Rio-Chanona, E. A.; Liu, J.; Wagner, J. L.; Zhang, D.; Meng, Y.; Xue, S.; Shah, N. Dynamic modeling of green algae cultivation in a photobioreactor for sustainable biodiesel production. *Biotechnology and Bioengineering* **2018**, *115*, 359–370.

(6)Juneja, A.; Ceballos, R. M.; Murthy, G. S. Effects of environmental factors and nutrient availability on the biochemical composition of algae for biofuels production: A review. *Energies* **2013**, *6*, 4607 – 4638.

(7)Acién, F. G.; Gómez-Serrano, C.; Morales-Amaral, M. M.; Fernández-Sevilla, J. M.; Molina-Grima, E. Wastewater treatment using microalgae: how realistic a contribution might it be to significant urban wastewater treatment? *Applied Microbiology and Biotechnology* **2016**, *100(21)*, 9013 – 9022.

(8)Costache, T. A.; Acién, F. G.; Morales, M. M.; Fernández-Sevilla, J. M.; Stamatin, I.; Molina, E. Comprehensive model of microalgae photosynthesis rate as a function of culture conditions in photobioreactors. *Applied Microbiology and Biotechnology* **2013**, *97(17)*, 7627–7637.

(9)Del Rio-Chanona, E. A.; Cong, X.; Bradford, E.; Zhang, D.; Jing, K. Review of advanced physical and data-driven models for dynamic bioprocess simulation: Case study of algae-bacteria consortium wastewater treatment. *Biotechnology and Bioengineering* **2019**, *116*, 342–353.

(10)Pawlowski, A.; Mendoza, J. L.; Guzmán, J. L.; Berenguel, M.; Acién, F. G.; Dormido, S. Selective pH and dissolved oxygen control strategy for a raceway rector within an event-based approach. *Control Engineering Practice* **2015**, *44*, 209–218.

(11)Fernández, I.; Acién, F. G.; Guzmán, J. L.; Berenguel, M.; Mendoza, J. L. Dynamic model of an industrial raceway reactor for microalgae production. *Algal Research* **2016**, *17*, 67 – 78.

(12)Fernández, I.; Acién, F. G.; Berenguel, M.; Guzmán, J. L.; Andrade, G. A.; Pagano, D. J. A lumped parameter chemical-physical model for tubular photobioreactors. *Chemical Engineering Science* **2014**, *112*, 116 – 129.

(13)Béchet, Q.; Shilton, A.; Guieysse, B. Maximizing productivity and reducing environmental impacts of full-scale algal production through optimization of open pond depth and hydraulic retention time. *Environmental Science & Technology* **2016**, *50*, 4102 – 4110.

(14)Del Rio-Chanona, E. A.; Ahmed, N. R.; Wagner, J.; Lu, Y.; Zhang, D.; Jing, K. Comparison of physics-based and data-driven modelling techniques for dynamic optimisation of fed-batch bioprocesses. *Biotechnology and Bioengineering* **2019**, *116*, 2971–2982.

(15)James, S. C.; Boriah, V. Modeling algae growth in an open-channel raceway. *Journal of Computational Biology* **2010**, *17*, 895–906.

(16)Bernard, O.; Rémond, B. Validation of a simple model accounting for light and temperature effect on microalgal growth. *Bioresource Technology* **2012**, *123*, 520 – 527.

(17)Huesemann, M.; Crowe, B.; Waller, P.; Chavis, A.; Hobbs, S.; Edmundson, S.; Wigmosta, M. A validated model to predict microalgae growth in outdoor pond cultures subjected to fluctuating light intensities and water temperatures. *Algal Research* **2016**, *13*, 195 – 206.

(18)Ras, M.; Steyer, J. P.; Bernard, O. Temperature effect on microalgae: A crucial factor for outdoor production. *Reviews in Environmental Science and Bio/Technology* **2013**, *12*, 153 – 164.

(19)Singh, S. P.; Singh, P. Effect of temperature and light on the growth of algae species: A review. *Renewable and Sustainable Energy Reviews* **2015**, *50*, 431 – 444.

(20)Karemore, A.; Yuan, Y.; Porubsky, W.; Chance, R. Biomass and pigment production for *Arthrospira platensis* via semi-continuous cultivation in photobioreactors: Temperature effects. *Biotechnology and Bioengineering* **2020**, *117(10)*, 1–13.

(21)Bechet, Q.; Shilton, A.; Park, J. K.; Craggs, R. J.; Guieysse, B. Universal temperature model for shallow algal ponds provides improved accuracy. *Environmental Science and Technology* **2011**, *45*, 3702–3709.

(22)Béchet, Q.; Sialve, B.; Steyer, J. P.; Shilton, A.; Guieysse, B. Comparative assessment of evaporation models in algal ponds. *Algal Research* **2018**, *35*, 283 – 291.

(23)Marsullo, M.; Mian, A.; Ensinas, A. V.; Manente, G.; Lazzaretto, A.; Marechal, F. Dynamic modeling of the microalgae cultivation phase for energy production in open raceway ponds and flat panel photobioreactors. *Frontiers in Energy Research* **2015**, *3*, 41–59.

(24)Slegers, P. M.; Lösing, M. B.; Wijffels, R. H.; van Straten, G.; van Boxtel, A. B. Scenario evaluation of open pond microalgae production. *Algal Research* **2013**, *2*, 358–368.

(25)Guzmán, J. L.; Acién, F. G.; Berenguel, M. Modelling and control of microalgae production in industrial photobioreactors. *Revista Iberoamericana de Automática e Informática Industrial* **2020**, *00*, 1 – 5. Doi: 10.4995/riai.2020.7133.

(26)Barceló-Villalobos, M.; Gómez Serrano, C.; Sánchez Zurano, A.; Alameda García, L.; Esteve Maldonado, S.; Peña, J.; Acién, F. G. Variations of culture parameters in a pilot-scale thin-layer reactor and their influence on the performance of *Scenedesmus almeriensis* culture. *Bioresource Technology Reports* **2019**, *6*, 190 – 197.

(27)Fernández, I.; Acién, F. G.; Fernández, J. M.; Guzmán, J. L.; Magán, J. J.; Berenguel, M. Dynamic model of microalgal production in tubular photobioreactors. *Bioresource Technology* **2012**, *126*, 172 – 181.

(28)Duffie, J. A.; Beckman, W. A. Solar Engineering of Thermal Processes. *2nd ed. Wiley-Interscience* **1991**,

(29)Praveen-Eluripati, R. An Improved Model for Estimating Evaporation over Lakes and Ponds. *Thesis submitted to the Graduate Faculty of the University of New Orleans* **2007**, *https://scholarworks.uno.edu/cgi/viewcontent.cgi?article=1567&context=td*.

(30)Sartori, E. A critical review on equations employed for the calculation of the evaporation rate from free water surfaces. *Solar Energy* **2000**, *68*, 77–89.

(31)Monteith, J. L.; Unsworth, M. H. Principles of Environmental Physics. *Third Ed. AP, Amsterdam* **2008**,

(32)Tetens, O. Über einige meteorologische Begriffe. *Z. Geophys* **1930**, *6*, 207–309.

(33)Houck, C.; Joines, J.; Kay, M. A Genetic Algorithm for Function Optimization: A Matlab Implementation. *NCSUIE-TR-95-09. North Carolina State University, Raleigh, NC, USA* **1998**, *22*.

(34)Camacho-Rubio, F.; García-Camacho, F.; Fernández-Sevilla, J. M.; Chisti, Y.; Molina Grima, E. A mechanistic model of photosynthesis in microalgae. *Biotechnology and Bioengineering* **2003**, *81(4)*, 459 – 473.

(35)Grima, E. M.; Fernández Sevilla, J. M.; Sánchez Pérez, J. A.; Garcia Camacho, F. A study on simultaneous photolimitation and photoinhibition in dense microalgal cultures taking into account incident and averaged irradiances. *Journal of Biotechnology* **1996**, *45(1)*, 59–69.